Deformations in (Al,Ga)As epitaxial layers wafer bonded on dissimilar substrates

B. Jenichen,[a] V. M. Kaganer, A. Riedel, H. Kostial, Q. Gong, R. Hey, K. Friedland, and K. H. Ploog
Paul-Drude-Institut für Festkörperelektronik, Hausvogteiplatz 5-7, D-10117 Berlin, Germany

(Received 24 July 2000; accepted for publication 22 November 2000)

Deformations in heteroepitaxial layer stacks of AlGaAs/GaAs grown on GaAs are measured by triple crystal diffractometry before epitaxial liftoff and after subsequent wafer bonding on various substrates (GaAs, glass, Si, and $LiNbO_3$). The tetragonal deformation present in the as-grown layer stack partially relaxes during epitaxial liftoff. The roughness of the as-grown layer stack gives rise to a bending of the atomic planes after wafer bonding. The widths of the x-ray diffraction peaks are used to estimate the misorientation of the lattice planes and compared with the atomic force microscopy measurements of the surface roughness. © *2001 American Institute of Physics.* [DOI: 10.1063/1.1342804]

I. INTRODUCTION

The technique of wafer bonding[1–9] releases the restrictions of lattice matching imposed by epitaxial growth and opens new degrees of freedom for the design of semiconductor devices, since the combination of unique properties of different materials becomes possible. This technique brings clean and flat surfaces of two wafers into close proximity. Attractive forces pull them together, forming an intimate contact between different materials. The strength of the adhesion depends on the type of interaction. van der Waals forces provide the first step of attraction. The bonding strength can be increased in materials with similar thermal expansion coefficients by an appropriate heat treatment, leading to the additional formation of covalent bonds across the bonding interface. Next, one of the wafers is thinned to obtain the required layer thickness for electronic or optical applications. Nearly perfect interfaces with regular dislocation arrays were found as the result of bonding of Si wafers.[1–4]

Combining wafer bonding with epitaxial lift-off techniques[5–7] opens additional possibilities. In this method, an epitaxial layer stack is grown on an appropriate substrate. Then, a thin sacrificial layer is removed by etching, in order to lift off the epitaxial layers from the substrate. The structure is transferred onto a new substrate by wafer bonding via van der Waals forces. The interfaces obtained by wafer bonding after epitaxial liftoff often have a less perfect geometry since high temperature thermal treatment is not performed.

High resolution x-ray measurements are well suited for the measurement of deformations in wafer bonded structures. X-ray measurements before and after the epitaxial liftoff of InAs layers on relaxed AlSb buffer layers from the GaAs substrate and subsequent bonding to glass[6] revealed a shift of the InAs peak. The shift was attributed to relaxation of residual stress. (Originally the lateral lattice parameter of the InAs layer matched that of the AlSb buffer removed during the process.) The introduction of additional in-plane strain into a GaAs/AlGaAs multiquantum well bonded to $LiNbO_3$ was observed and explained by the differences in thermal expansion coefficients.[7]

Wafer bonding for the Si on insulator technology was investigated by x-ray topography.[8] Voids were detected at the interface. The strain pattern found in the bonded areas was assumed to originate from variations in local flatness.[9] This effect has been correlated with optical profilometry measurements.

We explore the material combination of III–V heterostructures grown originally on GaAs with other substrates like $LiNbO_3$, glass, and Si. Epitaxial films (we use hereafter the words ''layer stack'' and ''film'' interchangeably) are removed from the original GaAs substrate by means of epitaxial liftoff and transferred to substrates using wafer bonding. In particular, the use of $LiNbO_3$ as a substrate allows for the combination of excellent electronic and optical properties of the epitaxial layer structures with acoustic properties of $LiNbO_3$. We investigate the deformation fields in the structures by triple crystal x-ray diffractometry before epitaxial liftoff and after wafer bonding. In addition, the surface roughness is measured by atomic force microscopy (AFM). We find that the deformations introduced by the wafer bonding mainly consist of additional bending of the film which is caused by a partial adaptation of its lower surface (which has a finite roughness) to the substrate.

II. EXPERIMENT

The films containing a modulation-doped GaAs quantum well with short-period superlattice barriers were grown by molecular beam epitaxy (MBE).[10] Figure 1 shows a schematic view of the structure as grown on a (001) GaAs substrate. The 10 nm thick GaAs quantum well (QW) was grown between two short-period superlattices (SPSL). The lower SPSL consists of 60 periods of 1.3 nm AlAs and 2.6 nm GaAs, the upper has only eight such periods. The top of

[a]Electronic mail: jen@pdi-berlin.de

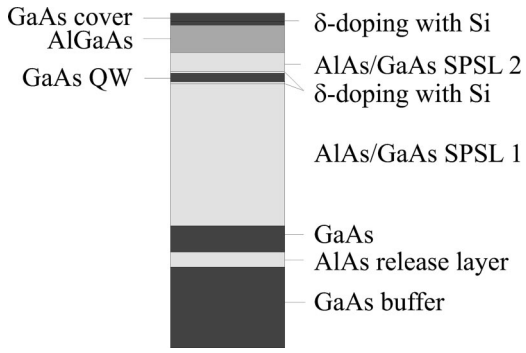

FIG. 1. Schematic view of the sample with a 10 nm thick GaAs QW grown between two short period superlattices (SPSL 1,2) on GaAs (001).

the film contains a 60 nm $Al_xGa_{1-x}As$ layer with $x=0.22$ and then a 20 nm GaAs cover layer. The cover layer and both the SPSL contain δ-doping Si layers. The AlAs release layer, grown between two thick GaAs layers, was etched away during epitaxial liftoff. The thickness of the epitaxial film above the release layer amounts to 375 nm.

The technology of epitaxial liftoff and wafer bonding follows Ref. 11 and is demonstrated in Fig. 2. A 50 nm AlAs layer serves as release layer. After wax coating, the sample is dipped into 10 wt% HF acid. The etch selectivity of AlAs with respect to GaAs is $\sim 10^8$. Although the SPSL contain very thin AlAs layers, the effective Al content of the superlattices is near 30%. The observed etch rate of the superlattices is many orders of magnitude lower than that of pure AlAs. The wax is utilized to induce strain, thus to increase the separation between the film and the GaAs substrate as the etching proceeds. As a result, the etchant inflow and the removal of etching products are enhanced. The temperature of the HF acid is 0 °C to avoid H_2 gas bubbles which disturb the homogeneous release etching. After removal from the substrate, the very fragile film is dipped into clean water and then transferred onto the cleaned substrate. Crucial for this process is a thin water layer remaining on the freshly etched epitaxial film, since its surface tension pulls the layer smooth. Drying at 80 °C for 30 min and using a weight of about 30 g/cm^2 to press the film on the new substrate completes the process. Crystallographic orientations of the surfaces of the new substrates were (001) for Si and GaAs, but (10.0) for $LiNbO_3$. The bonded area amounts to 0.25–0.5 cm^2. The bonding forces are van der Waals forces. A further strengthening of these forces by annealing was proven to be impossible because of the big differences in the thermal properties of the materials. Mechanical damage of the layers is observed between 250 and 300 °C.

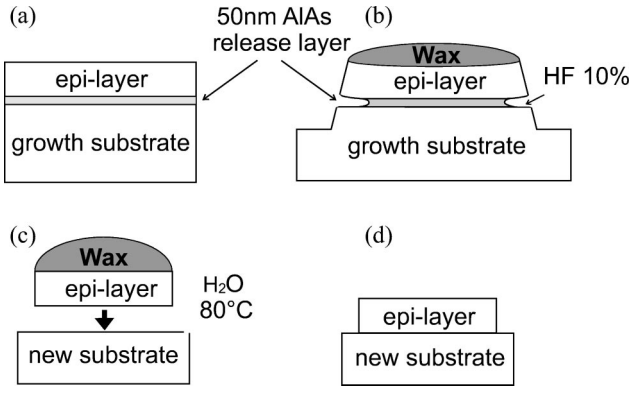

FIG. 2. Epitaxial liftoff technique: (a) growth of the epitaxial layer; (b) epitaxial liftoff by etching away a 50 nm AlAs thick release layer; (c) wafer bonding; (d) final structure.

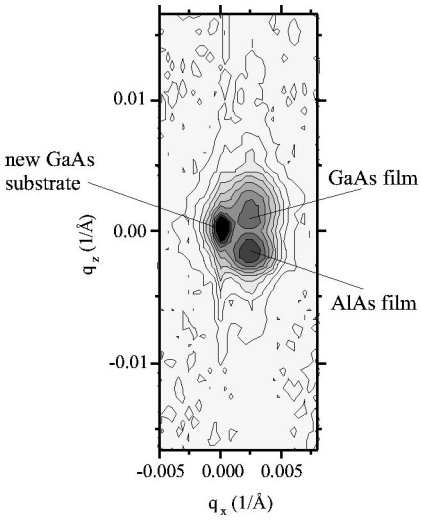

FIG. 3. Triple crystal area map of the sample bonded onto GaAs. The (004) diffraction peak of the GaAs substrate and two intensity maxima of the modulation doped quantum well structure are seen. The peaks of the film are shifted by the same amount of q_x with respect to the substrate peak due to the miscut of the substrate crystal of approximately 200″. The shift of the GaAs layer peak in q_z with respect to the GaAs substrate peak is due to stress relaxation inside the film after removal from the original substrate.

The original and the bonded samples were characterized by Hall measurements and high resolution x-ray diffraction in the triple crystal mode. A diffractometer with Du Mond–Bartels monochromator [symmetric Ge (220) reflection] and a channel-cut analyzer crystal [symmetric Si (111) reflection] was used. Diffraction curves were recorded near the symmetrical GaAs (004) and (002) reflections with Cu $K\alpha_1$ radiation. Simulations of the diffraction curves were performed in dynamical approximation.[12]

III. RESULTS

Figure 3 shows an example of the area map near the GaAs (004) reflection of the layer stack lifted off from the initial GaAs substrate and bonded onto another GaAs substrate. The substrate reflection near $(q_x,q_z)=(0,0)$ Å^{-1} and the two maxima of the film near $(q_x,q_z)=(0.0025, \pm 0.002)$ Å^{-1} are clearly distinguished. Here q_x and q_z are the deviations of the scattering vector from the Bragg maximum in directions parallel and perpendicular to the sample surface, respectively. The maxima of the film are shifted along q_x with respect to the substrate peak due to different miscuts of the substrate crystals used for the growth and the wafer bonding. The shift in q_z shows that the GaAs layers of the film do not have the same lattice parameter as the new GaAs substrate, because the stresses in the film are relaxed after epitaxial liftoff and tetragonal deformation is introduced in the thin GaAs layers of the stack.

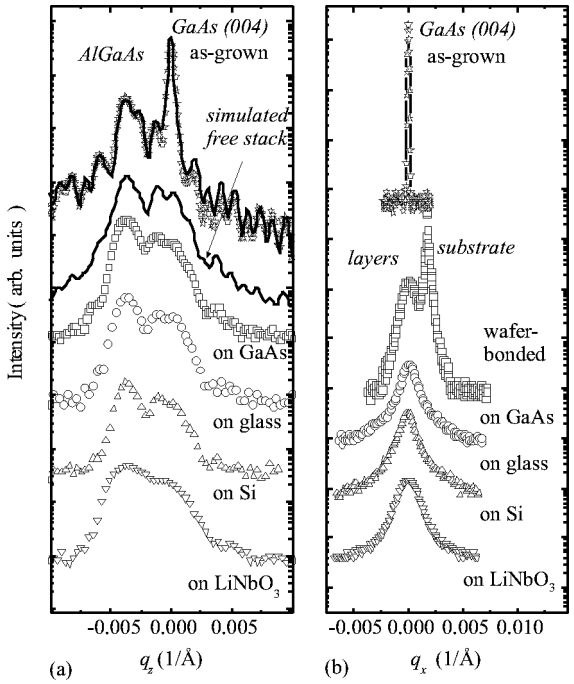

FIG. 4. Comparison of the triple-crystal q_z scans (a) and q_x scans (b) of the samples with epitaxial layer stacks: as-grown (stars) and bonded onto the different substrate materials GaAs (squares), glass (circles), Si (triangles up), and $LiNbO_3$ (triangles down). The full lines in (a) are simulations. The GaAs (004) reflection with Cu $K\alpha_1$ radiation was used.

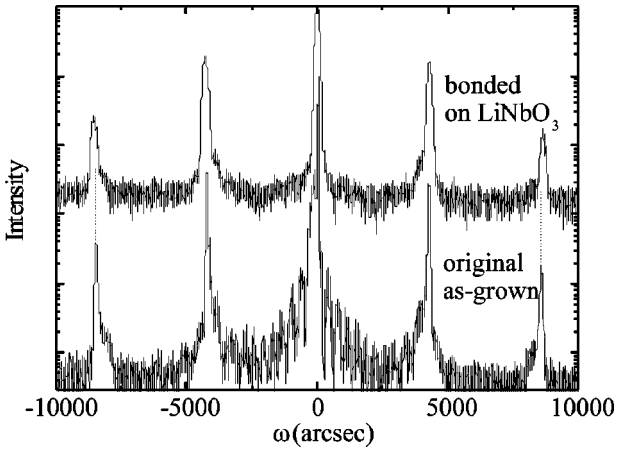

FIG. 5. Double crystal diffraction curves of the modulation doped quantum well structure bonded onto $LiNbO_3$ (upper curve) and of the original as-grown sample (lower curve). The GaAs(002) reflection with Cu $K\alpha_1$ radiation was used. Superstructure maxima due to the SPSLs inside the film are clearly visible. The distance between them is increased after epitaxial liftoff and wafer bonding on the $LiNbO_3$ substrate, indicating a shortening of the superlattice period by 0.26%.

In Fig. 4(a), the q_z scans are depicted before epitaxial liftoff (stars) and after wafer bonding to different substrates (open symbols): GaAs, glass, Si, and $LiNbO_3$. The spacings between the GaAs substrate peak and the average lattice peak of the film as grown on GaAs remain unchanged. In the simulations shown by lines in Fig. 4(a), fully strained structures (without misfit dislocations) are assumed. Figure 4(b) shows a comparison of the q_x scans of the structure as grown and bonded onto different substrates. The angular widths for the as-grown sample and the samples bonded on $LiNbO_3$ and glass are given in Table I. In addition the samples bonded on Si and GaAs showed misorientations σ/ξ of 1.71×10^{-4} and 1.65×10^{-4}, respectively. The broadening of the diffraction maxima is similar for the Si, glass, and the GaAs substrates and it is larger for $LiNbO_3$.

The stress present in the original layers due to the matching of the in-plane lattice parameters to that of the GaAs substrate relaxes in a way that the peak separation between the AlAs and GaAs peaks remains nearly unchanged [see Fig. 4(a)], i.e., the tetragonal deformation in the AlAs (originally under compression) reduces, while the GaAs layers become tensile stressed. This results in an opposite tetragonal deformation of the GaAs cell. The elastic relaxation of the film reduces the thicknesses of the AlAs as well as the GaAs layers. This effect can be detected with high accuracy by measuring the period of the short period AlAs/GaAs superlattices inside the sample (see Fig. 1). Figure 5 shows double crystal measurements near the GaAs (002) reflection for the as-grown layer stack and the film bonded onto $LiNbO_3$. Satellite reflections of the SPSLs are clearly visible. Compared with the as-grown film, the bonded one exhibits slightly broadened satellite reflections with an increased distance between them, indicating a shortening of the superlattice period by 0.26%. Care was taken in order to exclude the influence of the sample miscut on the distance of the satellite peaks by comparing measurements at different azimuths.

Figure 6 shows the surface topography of the original sample imaged by means of AFM. These measurements give the root mean square (rms) surface roughness σ_s of about 0.4 ± 0.1 nm with a lateral correlation length ξ_s of 1500 ± 500 nm. The AFM values were checked on the same sample by x-ray reflectivity and diffuse scattering measurements like in Refs. 13,14, which yielded $\xi_s=1570$ nm with a vertical correlation of the roughness over the whole film. The average

TABLE I. Rms surface roughness σ_s, its lateral correlation length ξ_s determined from the atomic force micrographs, the surface misorientation σ_s/ξ_s, and the misorientation of the lattice planes originally parallel to the surface σ/ξ as given by FWHM of the q_x scans in the x-ray scattering measurements, Eq. (7). The mobility of the two-dimensional electron gas μ and the carrier concentration n are added.

	AFM			X-ray	Hall effect	
Sample	σ_s [nm]	ξ_s [nm]	σ_s/ξ_s ($\times10^{-4}$)	σ/ξ ($\times10^{-4}$)	μ [m^2/Vs]	n [$10^{16}m^{-2}$]
as-grown	0.4 ± 0.1	1500 ± 500	2.67	⋯	128	0.99
on $LiNbO_3$	0.3 ± 0.1	1150 ± 500	2.61	2.21	121	1.01
on glass	0.4 ± 0.1	1200 ± 500	2.33	1.62	119	1.01

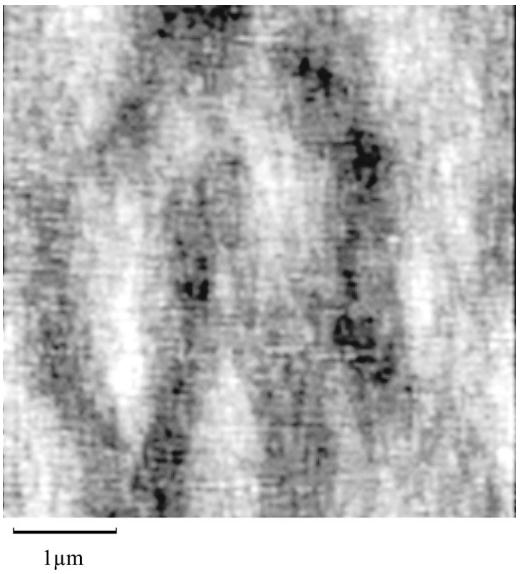

FIG. 6. Atomic force micrograph of the surface of the as-grown sample.

roughness amplitude σ_s was 0.4 ± 0.1 nm. Such values are typical for state of the art MBE growth of AlAs/GaAs layer systems on GaAs. The AFM data obtained for the bonded films (see Table I) reveal similar values of σ_s and ξ_s. Substrate surface roughnesses were also checked by AFM. Whereas GaAs, Si, and glass show roughnesses near 0.5 nm the $LiNbO_3$ exhibits a larger surface rouhgness of about 1.0 nm. This larger σ_s seems to be the reason for the observed extensive broadening of the layer reflection after bonding on $LiNbO_3$.

The structures exhibit extremely high two-dimensional electron densities n up to $1.6\times10^{16}\ m^{-2}$ and mobilities μ up to 130 $m^2/(V\,s)$. The δ-doping of the SPSL barrier creates X-electron gas, which is able to screen the potential fluctuations caused by the inhomogeneous distribution of the doping atoms, thereby improving the mobility of the electrons.[5] We could show, that those X electrons can be used also to screen the defects, which arise at the new interface as a result of the wafer bonding process. The high density as well as the high mobility are preserved after epitaxial liftoff and wafer bonding onto the new substrates (see Table I).

IV. DEFORMATIONS IN BONDED FILMS AND X-RAY DIFFRACTION PEAK WIDTHS

Figure 7 shows an idealized model of the epitaxial film decoupled from its growth substrate, Fig. 7(a), and after the bonding, Fig. 7(b). After the film is lifted off, its misfit strains are relaxed. The average roughness of the upper and lower film surfaces is the same as that of the as-grown surface. The rms roughness and the correlation length of the surface roughness of the free film are denoted by σ_s and ξ_s, respectively. It follows from the x-ray measurements on the as-grown samples that the roughness of the two surfaces, as well as all interfaces inside the film, have approximately the same rms average and similar lateral correlation lengths of the roughness.

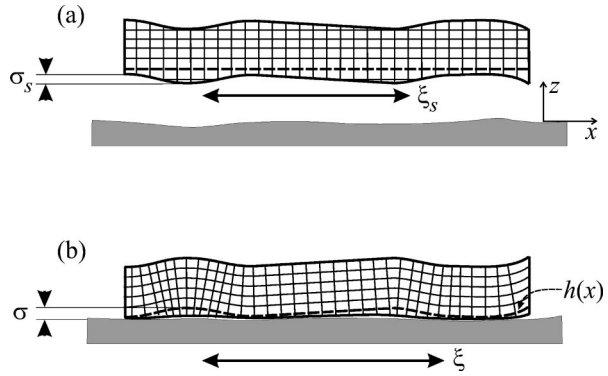

FIG. 7. A film lifted off (a) and subsequently bonded to a substrate (b). The roughness of the lower surface of the layer stack σ_s causes deformation gradients in the film, in particular, local bending with rms displacement σ near the interface. The deformations have a lateral correlation length ξ comparable to that of the original surface roughness ξ_s of the film.

When the film is bonded onto the substrate, Fig. 7(b), its surface is deformed due to the van der Waals attraction to the substrate. The elastic strains appearing in the bulk of the film cause broadening of the x-ray diffraction peaks. We select an atomic plane close to the interface [it is shown by broken lines in Figs. 7(a) and 7(b)] and denote its displacement due to film bonding by $h(x)$. This quantity can be considered, similarly to the common treatment of rough surfaces, as a Gaussian random function with a mean-square σ and a correlation length ξ. In the limiting case of an elastically soft film on a rigid smooth substrate, the parameters σ and ξ coincide with the corresponding values σ_s and ξ_s of the as-grown film. In the opposite limit of a rigid film on a soft substrate, the film is not deformed at all ($\sigma\to0$, $\xi\to\infty$). Generally, the roughness of the lattice planes inside the film σ,ξ does not coincide with the surface roughness σ_s,ξ_s.

The x-ray diffraction intensity from the strained film can be written as

$$I(q_x,q_z)=\int_{-\infty}^{\infty}dx dx'\int_0^t dz dz' e^{iq_x(x-x')}e^{iq_z(z-z')}e^{-T}, \tag{1}$$

where the correlation function is

$$e^{-T(x-x',z,z')}=\langle e^{i\mathbf{Q}\cdot[\mathbf{u}(x,z)-\mathbf{u}(x',z')]}\rangle. \tag{2}$$

The integrations over x and x' in Eq. (1) are performed in the infinite limits while the integrations over z and z' are limited by the thickness t of the film. The system is translationally invariant in the plane of the interface but not normal to it. Hence, the correlation function depends on the difference $x-x'$ and on z and z' separately. The intensity I depends on the wave vector deviations q_x,q_z from the Bragg point in the scattering plane. We take into account that, in the triple-crystal diffraction experiment, the divergence of the beams normal to the scattering plane is large, which leads to the integration of the intensity $\mathcal{I}(q_x,q_y,q_z)$ over q_y and selects the plane $y=0$ in the correlation function (2). We choose, in accordance with the experiment, the diffraction vector $\mathbf{Q}$ to be normal to the film. Then, only the normal component u_z of the displacement vector $\mathbf{u}(x,z)$ is of interest, one has $\mathbf{Q}\cdot\mathbf{u}=Qu_z$.

In the simplest approximation of a thin film, $t \ll \xi$, the displacement in the film does not depend on z and repeats the displacement at the interface, i.e., $u_z(x,z) \approx h(x)$. Then, the correlation function (2) is calculated as

$$T(x-x') = \tfrac{1}{2} Q^2 \langle [h(x) - h(x')]^2 \rangle. \tag{3}$$

The correlation function does not depend on z and z' and the corresponding integrals in Eq. (1) give a term $4q^{-2} \sin^2(q_z t/2)$. The diffraction peak is not broadened in the q_z direction compared to the undistorted film. The limit $x - x' \to \infty$ gives rise to the coherent component of the intensity equal to

$$I_{\mathrm{coh}} = \exp(-T_\infty)\, \delta(q_x) \frac{4 \sin^2(q_z t/2)}{q_z^2}, \tag{4}$$

where $\exp(-T_\infty)$ is the Debye–Waller factor, $T_\infty = Q^2 \sigma^2/2$, and $\sigma = \langle [h(x)]^2 \rangle^{1/2}$ is the rms roughness. The reciprocal-lattice vector Q entering the Debye–Waller factor in the present problem is much larger than typical z components of the wave vectors entering similar formula in the surface roughness studies at grazing incidence. Taking the measured value of the rms roughness of the as-grown film $\sigma_s = 0.4$ nm, we find $Q\sigma_s \approx 18$ for the GaAs(004) reflection and the Debye–Waller factor $\exp(-Q^2\sigma_s^2/2) \approx 10^{-34}$. The roughness of the lattice planes in the bonded film σ is comparable with σ_s, which explains the absence of the coherent peak from the bonded film in the experiment, Fig. 3.

The calculations of the correlation function (3) for finite $x - x'$ can be simplified by noting that only small values $|x - x'| \ll \xi$ are essential in the integral (1). We first expand $h(x) - h(x')$ in Eq. (3) up to the linear term and then prove that such expansion is sufficient

$$\begin{aligned} T(x-x') &\approx \tfrac{1}{2} Q^2 (x-x')^2 \langle (\partial h/\partial x)^2 \rangle \\ &= -\tfrac{1}{2} Q^2 (x-x')^2 \left. \frac{\partial^2 G(x)}{\partial x^2} \right|_{x=0}. \end{aligned} \tag{5}$$

The second derivative of the height-height correlation function $G(x-x') = \langle h(x) h(x') \rangle$ can be estimated as $-2(\sigma/\xi)^2$, since $G(x=0) = \sigma^2$ and the characteristic width of $G(x)$ is the correlation length ξ. Then, the range of $x - x'$ essential for the calculation of the integral (1) is $|x - x'| \sim \xi/(Q\sigma) \ll \xi$, since $Q\sigma \gg 1$, as discussed above. Calculating the Gaussian integral in Eq. (1), we find

$$I(q_x, q_z) = \frac{4 \sin^2(q_z t/2)}{q^2} \exp(-q_x^2/q_0^2), \tag{6}$$

where $q_0 = 2Q\sigma/\xi$. The x-ray diffraction peak described by Eq. (6) is broadened, compared to a free-standing film, only in the q_x direction, and has a full width half maximum (FWHM) of

$$\Delta q_x \approx 4 \sqrt{\ln 2}\, Q\sigma/\xi. \tag{7}$$

The qualitative interpretation of this result is straightforward. The misorientation of atomic planes $\omega \sim \pm 2\sigma/\xi$ is given by the ratio of the height of the roughness σ to its lateral scale ξ. The corresponding width of the diffraction peak is $\Delta q_x \approx 2\omega Q$.

We explore now the general case, when the displacement in the film $u_z(x,z)$ does not coincide with that at the interface $h(x)$ because of the stress relaxation at the free surface of the film. We write

$$u_z(x,z) = \int_{-\infty}^{\infty} U(x-\zeta, z) h(\zeta)\, d\zeta, \tag{8}$$

thus introducing the function $U(x,z)$ which describes the z component of the displacement due to a point perturbation $h(x) = \delta(x)$. Then, the average over the Gaussian random function $h(x)$ in Eq. (2) gives

$$\begin{aligned} T(x-x', z, z') = \frac{Q^2}{2} \int_{-\infty}^{\infty} & [U(x-\zeta, z) - U(x'-\zeta, z')] \\ & \times [U(x-\zeta', z) - U(x'-\zeta', z')] \\ & \times G(\zeta - \zeta')\, d\zeta\, d\zeta'. \end{aligned} \tag{9}$$

We proceed to the Fourier transforms,

$$\begin{aligned} U(x,z) &= \frac{1}{2\pi} \int_{-\infty}^{\infty} u_k(z) e^{ikx} dk, \\ G(x) &= \frac{1}{2\pi} \int_{-\infty}^{\infty} g_k e^{ikx} dk, \end{aligned} \tag{10}$$

and obtain

$$\begin{aligned} T(x,z,z') = \frac{Q^2}{4\pi} \int_{-\infty}^{\infty} g_k \{ & [u_k(z) - u_k(z')]^2 \\ & - 2u_k(z) u_k(z') \cos kx) \}\, dk. \end{aligned} \tag{11}$$

In particular, the approximation of a thin layer repeating the shape of the interface, $u_z(x,z) = h(x)$, gives $u_k(z) = 1$ and reduces Eq. (11) to

$$T(x) = \frac{Q^2}{2\pi} \int_{-\infty}^{\infty} g_k (1 - \cos kx)\, dk, \tag{12}$$

which is the Fourier transform of Eq. (3).

The displacement $u_k(z) \cos kx$ is the solution of the elastic problem for a film with a given displacement on the lower surface (the film—substrate interface) $u_k(z=0) = \cos kx$ and a free upper surface. The problem can be solved using the Airy stress function (Ref. 15, Sec. 24). As an additional boundary condition, necessary to solve the problem, we assume that the x component of the displacement **u** vanishes at the interface. The solution is cumbersome and we present here only its expansion for the wavelengths large compared to the thickness of the film, $kt \ll 1$. It presents a correction to the initial approximation $u_k(z) = 1$ and is sufficient for the purposes of the present article

$$u_k(z) = 1 - \alpha k^2 z^2, \tag{13}$$

where $\alpha = \nu/[2(1-\nu)]$ and ν is the Poisson ratio. Substitution of this expression into Eq. (11) gives an integral $\int_{-\infty}^{\infty} k^4 g_k dk$, which is equal to $2\pi \partial^4 G(x)/\partial x^4|_{x=0}$ and can be estimated as $2\pi\sigma^2/\xi^4$. Then, we obtain instead of Eq. (6)

$$I(q_x,q_z)=t^2\exp(-q_x^2/q_0^2)\times\int_0^1 dz\,dz'\,e^{iq_z t(z-z')}e^{-W(z^2-z'^2)^2}, \quad (14)$$

where it is denoted

$$W=\tfrac{1}{2}(\alpha Q\sigma)^2(t/\xi)^4. \quad (15)$$

The intensity distribution (14) strongly depends on the ratio of the film thickness t to the roughness correlation length ξ. As far as $t\ll\xi$, the broadening of the diffraction peak in q_z direction is negligible and Eq. (14) reduces to Eq. (6). If the film thickness is comparable with the correlation length, $t\geqslant\xi$, the diffraction peak broadens. The integral in Eq. (14) can be easily calculated numerically.

Thus, the broadening of the x-ray diffraction peak in the q_x direction is caused by change in orientation of the atomic planes. It is given by the ratio of the characteristic height of the interface roughness σ to the roughness correlation length ξ, Eq. (7). The strain effect on the peak broadening in the q_z direction, additional to the peak width due to the finite film thickness, strongly depends on the ratio of the film thickness t to the roughness correlation length ξ and is controlled by the parameter W given by Eq. (15).

V. DISCUSSION

X-ray diffuse scattering measurements of the as-grown film show that the surface roughness is correlated vertically over the whole film at least for long lateral correlation lengths,[14] and hence the roughness measured by AFM on the upper surface of the original sample corresponds roughly to the roughness of lower interfaces. The lower surface of the film, after etching of the release layer, is bonded onto the substrate. The surface roughness of the bonded layers measured by AFM is of the same order of magnitude as that of the as-grown sample. The roughness of the lower surface of the film (the upper side of the new bonded interface) is the main cause of deformation gradients in the film (in particular, of local bending near the interface, see Fig. 7). These deformations have a lateral correlation length comparable to that of the original surface roughness of the film. We use the widths of the x-ray diffraction peaks in q_x scans, Fig. 4(b), to estimate the misorientation of the lattice planes σ/ξ from Eq. (7), see Table I. The values of σ/ξ are close to the misorientation σ_s/ξ_s of the surface of the as-grown sample determined by x-ray diffuse scattering and AFM. We conclude that the adaptation of the rough lower surface of the film to the substrate during wafer bonding results in a misorientation of *lattice planes* in the film comparable with the initial misorientation of the *surface* of the as-grown film (Fig. 7).

The shortening of the structures by 0.26% detected by the change in the distances between the superlattice maxima of the structure bonded on $LiNbO_3$ is a result of stress relaxation inside the film.

In a second approximation we can estimate the parameter W, Eq. (15), using the surface roughness parameters $\sigma_s=0.4$ nm and $\xi_s=1500$ nm, which gives $W\approx 0.18$. Such small value of W does not cause any noticeable broadening of the x-ray diffraction peak in the q_z direction. The peak broadening for the film bonded on the $LiNbO_3$ substrate (Fig. 4) indicates a much larger strain gradient in the film. The film bonded on the $LiNbO_3$ substrate shows in addition somewhat larger, compared to the other substrates, broadening of the diffraction peak in the q_x-scan, Fig. 4, and somewhat smaller roughness correlation length measured by AFM (see Table I). The origin of this extensive broadening lies in the higher surface roughness of $LiNbO_3$ substrates.

VI. CONCLUSIONS

Deformation fields in epitaxial layer stacks were measured before epitaxial liftoff and after subsequent wafer bonding onto different templates. The stresses present in the original layers due to the matching of the lattice parameters parallel to the interface to that of the substrate relax, leaving the angular spacing between the AlAs and GaAs x-ray diffraction peaks nearly unchanged, i.e., the tetragonal deformation in the AlAs layers reduces but the GaAs layers also become strained. A resulting shortening of the superlattice period of nearly 0.26% was observed for the structure bonded on $LiNbO_3$.

The rough lower surface of the film matched to the substrate by adhesion gives rise to a bending of the lattice planes in the film. The adaptation of the rough surface of the film to the substrate during wafer bonding causes a misorientation of the lattice planes in the film comparable with the initial surface misorientation of the as-grown film.

ACKNOWLEDGMENT

The authors thank M. Höricke for the MBE growth of the original sample.

[1] J. Eymery, F. Fournel, F. Rieutord, D. Buttard, H. Moriceau, and B. Aspar, Appl. Phys. Lett. **75**, 3509 (1999).
[2] D. Buttard, J. Eymery, F. Rieutord, F. Fournel, D. Lübbert, T. Baumbach, and H. Moriceau, Physica B **283**, 103 (2000).
[3] P. B. Howes, M. Benamara, F. Grey, R. Feidenhansl, M. Nielsen, F. B. Rasmussen, and J. Baker, Physica B **248**, 74 (1998).
[4] Q.-Y. Tong and U. Gösele, *Semiconductor Wafer Bonding* (Wiley, New York, 1999).
[5] M. Msall, W. Dietsche, K.-J. Friedland, and Q. J. Tong, Phys. Rev. Lett. **85**, 598 (2000).
[6] C. Fastenau, E. Oezbay, G. Tuttle, and F. Laabs, J. Electron. Mater. **24**, 757 (1995).
[7] J. H. Lin *et al.*, Mater. Res. Soc. Symp. Proc. **356**, 331 (1995).
[8] W. P. Maszara, B. L. Jiang, A. Yamada, G. A. Rozgonyi, H. Baumgart, and A. J. R. de Kock, J. Appl. Phys. **69**, 257 (1991).
[9] H. Baumgart, T. J. Letavic, and R. Egloff, Philips J. Res. **49**, 91 (1995).
[10] K. J. Friedland, R. Hey, H. Kostial, R. Klann, and K. H. Ploog, Phys. Rev. Lett. **77**, 4616 (1996).
[11] E. Yablonovitch, T. Gmitter, J. B. Harbison, and R. Bhat, Appl. Phys. Lett. **51**, 2222 (1987).
[12] B. Rosner, PhD thesis, Humboldt-Universtät Berlin, 1990; W. J. Bartels, Inst. Phys. Conf. Ser. **87**, 599 (1987); S. Takagi, Acta Crystallogr. **15**, 1131 (1962); D. Taupin, Bull. Soc. Fr. Mineral. Cristallogr. **87**, 469 (1964).
[13] S. K. Sinha, Physica B **173**, 25 (1991).
[14] B. Jenichen, R. Hey, M. Wassermeier, and K. H. Ploog, Il Nuovo Cimento **19D**, 429 (1997).
[15] S. P. Timoshenko and J. N. Goodier, *Theory of Elasticity* (McGraw-Hill, New York, 1970).